Generalized correlation functions for conductance fluctuations and the mesoscopic spin Hall effect

J. G. G. S. Ramos,[1,2,3] A. L. R. Barbosa,[4] D. Bazeia,[2,5] M. S. Hussein,[1,2] and C. H. Lewenkopf[6]

[1]*Instituto de Estudos Avançados, Universidade de São Paulo, Caixa Postale 72012, 05508-970 São Paulo, São Paulo, Brazil*
[2]*Instituto de Física, Universidade de São Paulo, Caixa Postale 66318, 05314-970 São Paulo, São Paulo, Brazil*
[3]*Departamento de Ciências Exatas, Universidade Federal da Paraíba, 58297-000, Rio Tinto, Paraíba, Brazil*
[4]*UAEADTec and Pós-Graduação em Física Aplicada, Universidade Federal Rural de Pernambuco, 52171-900 Recife, Pernambuco, Brazil*
[5]*Departamento de Física, Universidade Federal da Paraíba, 58051-970 João Pessoa, Paraíba, Brazil*
[6]*Instituto de Física, Universidade Federal Fluminense, 24210-346 Niterói, Rio de Janeiro, Brazil*
(Received 19 July 2012; published 11 December 2012)

We study the spin Hall conductance fluctuations in ballistic mesoscopic systems. We obtain universal expressions for the spin and charge current fluctuations, cast in terms of current-current autocorrelation functions. We show that the latter are conveniently parametrized as deformed Lorentzian shape lines, functions of an external applied magnetic field and the Fermi energy. We find that the charge current fluctuations show quite unique statistical features at the symplectic-unitary crossover regime. Our findings are based on an evaluation of the generalized transmission coefficients correlation functions within the stub model and are amenable to experimental test.

I. INTRODUCTION

The discovery of the spin Hall effect (SHE)[1–4] in both metal and semiconductor structures has opened an important possibility to control the effects of nonequilibrium spin accumulation.[5] The basic idea underlying the SHE is to generate spin currents transverse to the longitudinal transport of charge by creating an imbalance between the spin-up and spin-down states.[6,7]

The detection of spin Hall conductance fluctuations is a major goal of semiconductor spintronics.[8] It is, however, a hard endeavor. The main reason is that the difficulty to efficiently connect ferromagnets leads to two-dimensional semiconductor structures.[9] For coupled metallic leads in ballistic systems, it is in principle possible to detect the signal when scattering by impurities induces a separation of the spin states.

Through this mechanism, universal spin Hall conductance fluctuations (USCFs) can lead to accumulation of spin at the electron reservoirs. The USCFs appear in the transverse current measured in multiterminal devices in the presence of a sufficiently large magnetic field.[6] Signals of the spin accumulation can be inferred, for instance, from time-dependent fluctuations of the spectral currents (noise power)[10] or from the analysis of universal conductance fluctuations.[11–14] Spin Hall conductance fluctuations have been theoretically studied for mesoscopic systems in the diffusive[11] as well as in the ballistic regime.[12] In the absence of both spin rotation symmetry and magnetic field, these studies predict universal spin Hall conductance fluctuations with a root-mean-square amplitude of about $0.18(e/4\pi)$.

So far, a direct detection of spin Hall currents by analyzing transverse current fluctuations has not been made. In this paper, we propose an alternative way to infer spin Hall conductance fluctuations, based on the universal relation between spin and charge current fluctuations in chaotic quantum dots. We find that the change and spin current-current correlation functions show a quite unique dependence on the ratio of open modes between transversal and longitudinal terminals. This dependence allows one to infer the magnitude of the spin current.

From the technical point of view, we adapt the diagrammatic technique developed to describe the electronic transport in two-terminal chaotic quantum dots in the presence of a spin-orbit interaction, at the symplectic-unitary crossover,[15,16] to the case of multiterminal spin-resolved currents.

The paper is organized as follows. In Sec. II we review the Landauer-Büttiker approach used to calculate the multiterminal charge and spin currents. Next, in Sec. III, we present the diagrammatic theory we employ to calculate the universal spin Hall current fluctuations. The phenomenological implications of our findings are discussed in Sec. IV. Finally, in Sec. V, we present our conclusions.

II. THEORETICAL FRAMEWORK

In this section we review the scattering matrix formalism that describes the spin Hall effect in ballistic conductors. We follow the approach put forward in Refs. 12, 17, and 18. We find helpful for the reader to have, in a nutshell, the expressions for the charge and spin currents with their explicit dependence on the electron energy and the presence of an external magnetic field. The latter is of particular importance in our study: The magnetic field breaks time-reversal symmetry and drives the symplectic-unitary crossover. The description of the universal spin current fluctuations at the crossover is one of the key results of this paper, as discussed in Sec. III.

We consider multiterminal two-dimensional systems where the electrons flow under the influence of a spin-orbit interaction of the Rashba and/or Dresselhaus type. The device is connected by ideal point contacts to $\mathcal{N}$ independent electronic reservoirs, denoted by $i = 1, \ldots, \mathcal{N}$. The electrodes are subjected to voltages denoted by V_i. We use the Landauer-Büttiker approach to write the α-direction spin-resolved current through the ith terminal as[19]

$$I_i^{\alpha\sigma} = \frac{e^2}{h} \sum_{j,\sigma'} \sum_{\substack{m\in i \\ n\in j}} \left| S_{m,\sigma;n,\sigma'}^{\alpha} \right|^2 (V_i - V_j), \qquad (1)$$

where σ and σ' are the spin projections in the $\alpha = x$, y, or z direction and S is the quaternionic scattering matrix of order $2N_T \times 2N_T$ that describes the transport of electrons through the system. The total number of open orbital scattering channels is $N_T = \sum_{i=1}^{\mathcal{N}} N_i$, where N_i is the number of open channels in ith lead point contact.

The electric current at the ith terminal is $I_i^{(0)} = I_i^{\alpha\uparrow} + I_i^{\alpha\downarrow}$ for any direction $\alpha = x,y,z$ of the electron spin projection. Similarly, the α-axis component of the spin current $I_i^{(\alpha)}$ is defined as the difference between the two spin projections along the α axis, namely, $I_i^{(\alpha)} = I_i^{\alpha\uparrow} - I_i^{\alpha\downarrow}$.

Let us consider a setup with $\mathcal{N} = 4$ terminals. An applied bias voltage between electrodes $i = 1$ and 2 gives rise to a longitudinal electronic current I and, due to the spin Hall effect, to spin currents at the transversal contacts.[11] Charge conservation imposes that $I \equiv I_1^{(0)} = -I_2^{(0)}$. Moreover, due to the absence of a transversal voltage bias, $I_i^{(0)} = 0$ for $i = 3,4$. Using these constraints, it was shown[12] that the transversal spin currents are given by

$$J_i^{(\alpha)} = \tfrac{1}{2}\left(\mathcal{T}_{i2}^{(\alpha)} - \mathcal{T}_{i1}^{(\alpha)}\right) - \mathcal{T}_{i3}^{(\alpha)}\widetilde{V}_3 - \mathcal{T}_{i4}^{(\alpha)}\widetilde{V}_4, \quad (2)$$

where $i = 3,4$. Likewise, the longitudinal charge current reads

$$J_i^{(0)} = \tfrac{1}{4}\left(2N_1 - \mathcal{T}_{11}^{(0)} + 2N_2 - \mathcal{T}_{22}^{(0)} + \mathcal{T}_{12}^{(0)} + \mathcal{T}_{21}^{(0)}\right) \\ - \tfrac{1}{2}\left(\mathcal{T}_{23}^{(0)} - \mathcal{T}_{13}^{(0)}\right)\widetilde{V}_3 - \tfrac{1}{2}\left(\mathcal{T}_{24}^{(0)} - \mathcal{T}_{14}^{(0)}\right)\widetilde{V}_4, \quad (3)$$

where $i = 1,2$. For notational convenience one introduces the dimensionless currents $J = h/e^2(I/V)$. The effective voltages $\widetilde{V}_i$ in volts, are given by rather lengthy expressions of the generalized transmission coefficients $\mathcal{T}_{ij}^{(0)}$, which can be found in Ref. 12. Finally, the generalized transmission coefficients read

$$\mathcal{T}_{ij}^{(\alpha)}(E,E',B,B') = \text{tr}[(1_i \otimes \sigma^\alpha)S^\dagger(E,B)1_j S(E',B')], \quad (4)$$

where E and B stand for the electron energy and the magnitude of an external magnetic field. The trace is taken over the scattering channels that belong to the ith and jth point contacts. The matrix 1_i stands for a projector of the scattering amplitudes into ith point contact channels. The matrices σ^α, with $\alpha \in \{x,y,z\}$, are the Pauli matrices, while σ^0 is the 2×2 identity matrix characterizing an unpolarized (charge) transport.

III. UNIVERSAL SPIN HALL CONDUCTANCE FLUCTUATIONS

We assume that the electron dynamics in the quantum dot is ballistic and ergodic,[20,21] and we model the system statistical properties using the random matrix theory (RMT). In this section, we describe the procedure to obtain universal spin and charge current-current autocorrelation functions given by Eqs. (2) and (3). We compare our analytical expressions with the results from numerical simulations.

Let us assume that spin-orbit interaction is sufficiently strong to fully break the system spin-rotational symmetry. In other words, the spin-orbit scattering time is much smaller than the electron dwell time in the system; that is, $\tau_{\text{so}} \ll \tau_{\text{dwell}}$. Hence, in the absence of an external magnetic field, the scattering matrix has symplectic symmetry. By increasing B, the system is driven through a crossover from the symplectic to the unitary symmetry.

The resonance S matrix can be parameterized as[22]

$$S(E,B) = TU[1 - Q^\dagger R(E,B)QU]^{-1}T^\dagger, \quad (5)$$

where U is a matrix of order $2M \times 2M$ of quaternionic form.[23] M stands for the number of resonances of the quantum dot. We take $M \gg N_T$. The matrices Q and T describe projector operators of order $(2M - 2N_T) \times 2M$ and $2N_T \times 2M$, respectively. Their matrix elements read $Q_{i,j} = \delta_{i+2N_T,j}$ and $T_{i,j} = \delta_{i,j}$. The matrix R of order $(2M - 2N_T) \times (2M - 2N_T)$ reads

$$R(\epsilon,x) = \exp\left(\frac{i\epsilon}{M}\sigma^0 + \frac{x}{M}X\sigma^0\right), \quad (6)$$

where X is an anti-Hermitian Gaussian distributed random matrix, while $\epsilon = (\tau_{\text{dwell}}/\hbar)E$ and $x^2 = \tau_{\text{dwell}}/\tau_B$ are dimensionless parameters representing E and B.

Both the dwell time τ_{dwell} and the magnetic scattering time τ_B are system-specific quantities. τ_{dwell} is usually expressed in terms of the decay width, namely $\Gamma = \hbar/\tau_{\text{dwell}} = N_T \Delta/2\pi$, where Δ is the system mean level spacing. In turn, τ_B^{-1} is the rate by which the electron trajectory accumulates magnetic flux in the quantum dot. For chaotic systems, $\tau_B^{-1} = \kappa(\mathcal{A}B)/\phi_0$, where ϕ_0 is the unit flux quantum, $\mathcal{A}$ is the quantum dot lithographic area, and κ is a diffusion coefficient that depends on the quantum dot geometry.[24]

The S matrix given by Eq. (5) can be formally expanded in powers of U, namely,

$$S(\epsilon,x) = \sum_{m=0}^{\infty} TU[Q^\dagger R(\epsilon,x)QU]^m T^\dagger,$$

and used to calculate the ensemble average of the transmission coefficients $\langle \mathcal{T}_{ij}^{(\alpha)} \rangle$ for $M \gg N_T$. Following this algebraic procedure, we write the sample transmission coefficient as a two-point function of the S matrix,

$$\mathcal{T}_{ij}^{(\alpha)}(\epsilon,\epsilon',x,x') = \sum_{m,n=0}^{\infty} \text{Tr}\{(1_i \otimes \sigma^\alpha)T[U^\dagger Q^\dagger R^\dagger(\epsilon,x)Q]^m \\ \times U^\dagger T 1_j T U[Q^\dagger R(\epsilon',x')QU]^n T^\dagger\}. \quad (7)$$

For chaotic quantum dots, as standard,[15] we assume the matrix elements of U as Gaussian variables, with zero mean and variance $1/M$. This allows one to express the calculation of moments and cumulants of $\mathcal{T}_{ij}^{(\alpha)}$ by an integration over the unitary group leading to a diagrammatic expansion in powers of N_T^{-1} in terms of diffuson (ladder) and cooperon (maximally crossed) diagrams. The method is described for the Dyson ensembles in Ref. 22. This approach has been extended to treat the crossover between symmetry classes[15,25] and is shown to render the same results as the quantum circuit theory.[25]

The diagrammatic technique[22] allows one to calculate moments up to arbitrary order of the transmission coefficients. It consists in grouping and integrating over the Haar measure all the independent powers of U in Eq. (7). Figure 1 shows the diagrams that represent the leading-order contributions to all possible contractions of the U matrices. In the sum of Eq. (7), we verify that, after taking the average over U, only the powers with $m = n$ contribute to the average transmission coefficients. The white and black dots in Fig. 1 stand for the indices of the matrix U, with elements U_{ij} in the channels space, while the
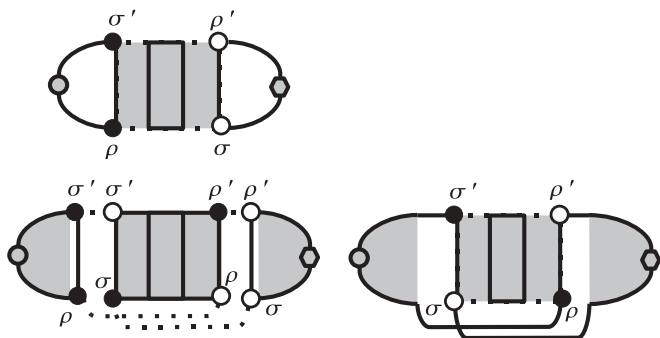
FIG. 1. Diagrams representing the leading contributions to the average transmission coefficient $\langle \mathcal{T}_{ij}^{(\alpha)} \rangle$ of Eq. (7). Vertical lines represent contractions of the U matrix elements. The white and black dots stand for the channel indices of the matrix U and the Greek symbols represent the Pauli matrix indices $\sigma_{\rho,\sigma}$ in the spin space. The first diagram (top) is known as the diffuson and accounts for the semiclassical diffusive processes. The two others diagrams are known as cooperons and give the mean quantum correction, namely, the weak (anti)localization corrections.

Greek symbols represent the Pauli matrix indices $\sigma_{\rho,\sigma}$ in the spin space.

The diagram at the top row of Fig. 1 is called a diffuson, in analogy to the ladder diagram that appears in diagrammatic expansion to calculate the conductivity in disordered diffusive mesoscopic systems.[26] The diffuson contribution to the average transmission coefficient reads

$$\left\langle \mathcal{T}_{ij}^{(\alpha)}(\epsilon,\epsilon',x,x') \right\rangle^{(d)} = \frac{1}{2} \sum_{\rho\sigma} [\mathrm{Tr}(1_i \otimes \sigma^\alpha)\mathcal{D}\mathrm{Tr}(1_j) \\ - \mathrm{Tr}(1_i \otimes \sigma^\alpha)\mathcal{D}^2\mathrm{Tr}(1_j)]_{\rho\sigma;\sigma\rho}, \quad (8)$$

where, for clarity, we make explicit the spin degree of freedom of the symplectic structure. We use the properties $\mathrm{Tr}(1_i \otimes \sigma^\alpha) = 2N_i\delta_{\alpha0}$ and $\mathrm{Tr}(1_j) = 2N_j$ to write

$$\mathcal{D}^{-1} = 2M\sigma^0 \otimes \sigma^0 - \mathrm{Tr}(R \otimes R'^\dagger) \quad (9)$$

with

$$\mathrm{Tr}(R \otimes R'^\dagger) \\ = \sigma^0 \otimes \sigma^0[2M - 2N_T - 2i(\epsilon - \epsilon') - (x - x')^2], \quad (10)$$

where R' is a shorthand notation for $R(\epsilon',x')$. The tensor products follow the "backward algebra,"[15,16] namely, $(\sigma^i \otimes \sigma^j)(\sigma^k \otimes \sigma^l) = (\sigma^i\sigma^k) \otimes (\sigma^l\sigma^j)$.

The diffuson contribution to the generalized transmission coefficient is obtained by evaluating Eq. (8) using expressions (9) and (10). It reads

$$\left\langle \mathcal{T}_{ij}^{(\alpha)}(\epsilon,\epsilon',x,x') \right\rangle^{(d)} = \delta_{\alpha0} \frac{N_i N_j}{N_D} \left(2 + \frac{1}{N_D} \right), \quad (11)$$

where $N_D = N_T[1 - i(\epsilon' - \epsilon) + (x' - x)^2/2]$.

We are now ready to evaluate the two maximally crossed diagrams at the bottom row of Fig. 1. They are known as cooperons[26] and represent the main quantum interference correction to the conductance in chaotic systems, responsible for the weak localization peak.

Following the procedure described above, we obtain the cooperon contribution for the generalized average

transmission, namely,

$$\left\langle \mathcal{T}_{ij}^{(\alpha)}(\epsilon,\epsilon',x,x') \right\rangle^{(c)} = \frac{1}{2} \sum_{\rho\sigma} \left[\mathrm{Tr}\left(F_i^{(\alpha)}(\mathcal{T} f_{TT}\mathcal{T})F_j \right) \right. \\ \left. - \frac{1}{(2M)^3}\mathrm{Tr}\left(F_i^{(\alpha)}(\mathcal{T} f_{TT}\mathcal{T}) \right)\mathrm{Tr}(F_j) \right]_{\rho\sigma;\rho\sigma}. \quad (12)$$

The operator $\mathcal{T} = \sigma^0 \otimes \sigma^y$ is related to the time-reversal of the path in the cooperon channel of the dual space. We also define the matrices

$$F_i^{(\alpha)} = 1_i \otimes \sigma^\alpha + \mathrm{Tr}(1_i \otimes \sigma^\alpha)\mathcal{D}(R'^\dagger \otimes R), \\ F_j = 1_j + \mathrm{Tr}(1_j)\mathcal{D}(R'^\dagger \otimes R), \quad (13)$$

where

$$f_{UU} = [2M\sigma^0 \otimes \sigma^0 - \mathrm{Tr}(R \otimes R^*)]^{-1}, \\ f_{TT} = (2M\sigma^0 \otimes \sigma^0)\mathrm{Tr}(R \otimes R'^*)f_{UU}. \quad (14)$$

The superscript $*$ denotes the quaternion complex conjugation. Using the quaternionic conjugation rules and taking the limit $M \to \infty$, we obtain

$$f_{UU}^{-1} = 2N_C\sigma^0 \otimes \sigma^0. \\ f_{TT} = (2M\sigma_0 \otimes \sigma_0)[(2M - 2N_C)\sigma_0 \otimes \sigma_0]f_{UU}, \quad (15)$$

where $N_C = N_T[1 - i(\epsilon' - \epsilon) + (x' + x)^2/2]$.

Summing up the diffuson and the cooperon contributions to the generalized transmission coefficients, we obtain

$$\left\langle \mathcal{T}_{ij}^{(\alpha)}(\epsilon,\epsilon',x,x') \right\rangle = \delta_{\alpha0} \left\{ \frac{2N_i N_j}{N_D} + \frac{N_i}{N_C} \right. \\ \left. \times \left[\frac{N_j[N_D + i(\epsilon - \epsilon')]}{N_D^2} - \delta_{ij} \right] \right\}. \quad (16)$$

For $\alpha = 0$, Eq. (16) reproduces the average electron transmission reported in the literature.[22] As expected in this case, the average spin transmission coefficients are zero.

Let us now analyze the transmission coefficient fluctuations. We use the same diagrammatic procedure described above for all the 32 diagrams characteristic of the usual covariance calculations.[22] To address relevant physical situations, it is sufficient to consider transmission coefficients with single energy and magnetic field arguments, that is, $\mathcal{T}_{ij}^{(\alpha)}(\epsilon,x) \equiv \mathcal{T}_{ij}^{(\alpha)}(\epsilon,\epsilon,x,x)$. Following the diagrammatic approach,[25] we calculate the covariance $\mathrm{cov}[\mathcal{T}_{ij}^{(\alpha)}(\epsilon,x),\mathcal{T}_{kl}^{(\beta)}(\epsilon',x')] \equiv \langle \mathcal{T}_{ij}^{(\alpha)}(\epsilon,x)\mathcal{T}_{kl}^{(\beta)}(\epsilon',x') \rangle - \langle \mathcal{T}_{ij}^{(\alpha)}(\epsilon,x) \rangle\langle \mathcal{T}_{kl}^{(\beta)}(\epsilon',x') \rangle$ and obtain

$$\mathrm{cov}\left[\mathcal{T}_{ij}^{(\alpha)}(\epsilon,x),\mathcal{T}_{kl}^{(\beta)}(\epsilon',x') \right] \\ = \delta_{\alpha0}\frac{N_i N_j N_k N_l}{N_T^2}\left(\frac{1}{|N_D|^2} + \frac{1}{|N_C|^2} \right) + \delta_{\alpha\beta}\frac{\delta_{ik}\delta_{jl}N_i N_j}{|N_D|^2} \\ + \delta_{\alpha0}\frac{\delta_{il}\delta_{jk}N_i N_k}{|N_C|^2} - \frac{N_i N_k}{N_T}\left(\delta_{\alpha0}\frac{\delta_{jl}N_j}{|N_D|^2} + \delta_{\alpha\beta}\frac{\delta_{ik}N_j N_l}{N_k|N_D|^2} \right. \\ \left. + \delta_{\alpha0}\frac{\delta_{jk}N_l + \delta_{il}N_j}{|N_C|^2} \right). \quad (17)$$

Support for our analytical findings is provided by numerical simulations. For that purpose, we find it convenient to

employ the Hamiltonian approach to the S matrix.[27] The latter is more amenable to numerical simulations than the S-matrix parametrization of Eq. (5) and both are statistically equivalent.[28]

The Hamiltonian parametrization of the S matrix reads

$$S(E,B) = \mathbb{1} - 2\pi i W^{\dagger}(E - H(B) + i\pi W W^{\dagger})^{-1} W, \quad (18)$$

where E is the electron propagation energy and $H(B)$ is the matrix of dimension $2M \times 2M$ that describes the resonant states (M orbital states times the two spin projections). In general, H depends on one or more external parameters. As discussed before, we are interested in the case where by increasing B one breaks time-reversal symmetry, driving the system from the symplectic to the unitary symmetry. In our numerical simulations, we consider $B \gg B_c$, namely, the specific case of pure ensembles. Accordingly, H is taken as a member of the Gaussian unitary ensemble corresponding to the case of broken time-reversal symmetry, usually denoted by $\beta = 2$. The matrix W of dimension $M \times (2N_T)$ contains the channel-resonance coupling matrix elements. Since the H matrix is statistically invariant under unitary transformations, the statistical properties of S depend only on the mean resonance spacing Δ, determined by H, and $W^{\dagger}W$. We assume a perfect coupling between channels and resonances, which corresponds to maximizing the average transmission following a procedure described in Ref. 29.

For simplicity, we take the case of $N \equiv N_i$. The results presented in Figs. 2 and 3 correspond to the systems with $N = 5$ perfectly coupled modes and $M = 400$ resonant levels. Hence, the S matrix has $2N_T = 40$ open channels. The ensemble averages are taken over $N_r = 10^5$ realizations within an energy interval around the band center, comprising about $M/4$ resonances.

Figure 2 compares the average transmission $\langle T_{ij}^{(\alpha)}(\epsilon) \rangle$ obtained from the numerical simulations with the analytical expression (16) for a number of different cases. The agreement
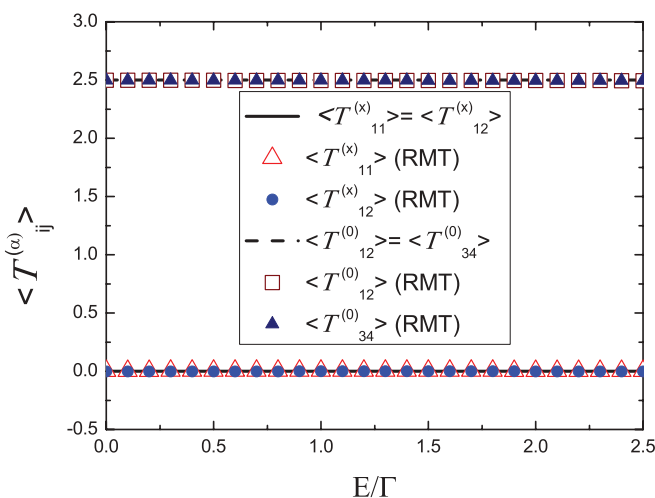

FIG. 2. (Color online) Generalized average transmission coefficient $\langle \mathcal{T}_{ij}^{(\alpha)}(\epsilon, x = 0) \rangle$ versus energy $\epsilon = E/\Gamma$ for different spin and terminal indices. The analytical results (stub model) are represented by the solid and dotted lines, while the results of numerical simulations (RMT Hamiltonian model) are represented by the symbols. The figure inset describes the different $\mathcal{T}_{ij}^{(\alpha)}$.
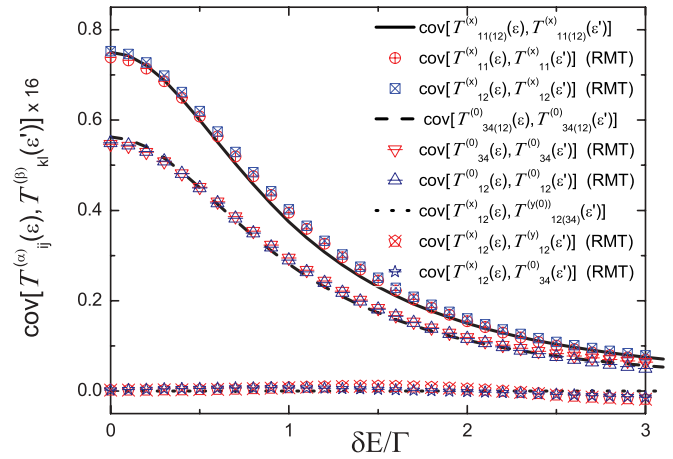

FIG. 3. (Color online) Transmission coefficient covariance $\mathrm{cov}[\mathcal{T}_{ij}^{(\alpha)}(\epsilon, x = 0)\mathcal{T}_{kl}^{(\beta)}(\epsilon', x = 0)]$ as a function of the energy difference $\Delta\epsilon = (E - E')/\Gamma$ for different spin and terminal indices. The analytical results (stub model) are represented by the solid and dotted lines, while the results of numerical simulations (RMT Hamiltonian model) are represented by the symbols. The figure inset describes the different $\mathrm{cov}[\mathcal{T}_{ij}^{(\alpha)}(\epsilon)\mathcal{T}_{kl}^{(\beta)}(\epsilon')]$ considered.

is very good, with accuracy of the order of $N_r^{-1/2}$. The simulations indicate that the average transmission is stationary in $\epsilon = E/\Gamma$, as it should be.

Figure 3 contrasts transmission coefficient covariances calculated using Eq. (17) with those obtained from numerical simulations for a number of different cases. As before, the discrepancies are very small and stay within the statistical precision $N_r^{-1/2}$. The random matrix theory[29] predicts an autocorrelation length $\Gamma = N_T \Delta/(2\pi)$ for a two-terminal geometry. Our results for the correlation function extend the latter to four-terminal geometries with (or without) spin polarization.

Let us now return to the calculation of spin and charge currents and effective voltages. As mentioned, those are combinations of transmission coefficients. Fortunately, it is possible to express average currents and current-current correlation functions in terms of the average transmission and the transmission-transmission correlation functions already analytically calculated and confirmed numerically. The effective voltages $\widetilde{V}_3$ and $\widetilde{V}_4$ show sample-to-sample fluctuations that depend both on the energy and on the magnetic field. On the other hand, as discussed in Ref. 12, their ensemble averages depend only on the number of open channels, namely, $\langle \widetilde{V}_i(\epsilon, x) \rangle = 1/2(N_1 - N_2)/(N_1 + N_2)$, with $i = 3, 4$. We also note that the ensemble average of the spin current is always zero, $\langle J_i^{(\alpha)}(\epsilon, x) \rangle = 0$, with $i = 3, 4$ and $\alpha \neq 0$, independently of the energy and magnetic field.

The USCFs do not depend on the device geometry (or on the positions of the terminals) but rather on the number of open channels at each terminal. Without loss of generality, let us analyze the spin current covariance for the case $N_1 = N_2 = N$ and $N_3 = N_4 = nN$, a setting that is easily realized in experiments. Here, n is a real positive number that we call the "channel factor."[30]

For the spin currents, for which $\alpha \neq 0$, we obtain

$$\mathrm{cov}[J_i^{(\alpha)}(\epsilon, x), J_i^{(\alpha)}(\epsilon', x')] = \frac{1}{8} \frac{n/(1+n)^2}{(1 + \delta x^2)^2 + \delta\epsilon^2}, \quad (19)$$

where $\delta\epsilon = \epsilon - \epsilon'$ and $\delta x = x - x'$. It is worth noticing that, for $n = 1$ and $\delta\epsilon = \delta x = 0$, Eq. (19) perfectly reproduces the recently reported results[11,12] for the universal fluctuations of the transverse spin conductance, namely, $\mathrm{rms}[G_{\mathrm{sH}}] = e/4\pi\{\mathrm{cov}[J_i^{(\alpha)}(\epsilon,x), J_i^{(\alpha)}(\epsilon,x)]\}^{1/2} \approx 0.18 e/4\pi$.

Equation (19) shows that the spin current correlation functions do not depend on the cooperon channels, that give rise to terms containing N_C. Hence, these quantities do not depend on the magnetic field, represented by x, but rather on its variations, δx. As a consequence, in the setup we consider, the spin current fluctuations are invariant in the symplectic-unitary crossover regime, a quite remarkable property.

The charge current fluctuations, on the other hand, depend on both the cooperon and diffuson channels, leading to

$$\mathrm{cov}[J_i^{(0)}(\epsilon,x), J_i^{(0)}(\epsilon',x')]$$
$$= \frac{1}{16}\left\{\frac{1+2n}{(1+n)^3}\frac{1}{(1+\delta x^2)^2 + \delta\epsilon^2}\right.$$
$$\left. + \frac{1}{(1+n)^2}\frac{1}{[1+(2x+\delta x)^2]^2 + \delta\epsilon^2}\right\}, \quad (20)$$

where $i = 1,2$. The magnetic field, represented by x, drives the symplectic-unitary crossover. For $x = 0$, one recovers the symplectic limit, while the unitary one is attained when $x \gg 1$. Note that in the absence of "transverse" leads, or $n = 0$, Eq. (20) reproduces the two-terminal result found in Ref. 15.

From Eq. (20) it follows that

$$\mathrm{cov}\{[J_i^{(0)}(\epsilon,x) - J_i^{(0)}(\epsilon,-x)]^2\} = \frac{16nx(1+2x^2)}{(1+n)(1+4x^2)^2}, \quad (21)$$

which demonstrates that, except for the two-terminal case where $n \neq 0$, the charge currents are not even functions of the magnetic field x.[19]

IV. ALTERNATIVE STATISTICAL MEASURES

Equations (19) and (20) are the main results of this paper. Unfortunately, the statistical sampling required to confirm our predictions for the dimensionless currents is rather large, making the experimental requirements quite daunting. An easier accessible statistical measure was recently proposed:[31] The dimensionless current $J_i^{(\alpha)}$ fluctuates as ϵ and x are varied. Let us call the external parameter z. Useful statistical information can be extracted from the number of maxima (or minima) of the $J_i^{(\alpha)}(z)$ in a given interval $[z, z + \delta z]$. Using a scale invariance and maximum entropy principle, we relate the joint probability of $J_i^{(\alpha)}(z)$ and its derivatives to a general equation for the density of maxima, for spin and/or charge transport. The average densities of maxima, $\langle\rho_z^{(\alpha)}\rangle$, of the fluctuating current $J_i^{(\alpha)}$ are given by[31]

$$\langle\rho_z^{(\alpha)}\rangle = \frac{1}{2\pi}\sqrt{\frac{T_4}{T_2}}$$
$$T_2 = -\frac{d^2}{d(\delta z)^2}\mathrm{cov}[J_i^{(\alpha)}(\epsilon,x), J_i^{(\alpha)}(\epsilon',x')]\big|_{\delta z = 0} \quad (22)$$
$$T_4 = \frac{d^4}{d(\delta z)^4}\mathrm{cov}[J_i^{(\alpha)}(\epsilon,x), J_i^{(\alpha)}(\epsilon',x')]\big|_{\delta z = 0},$$

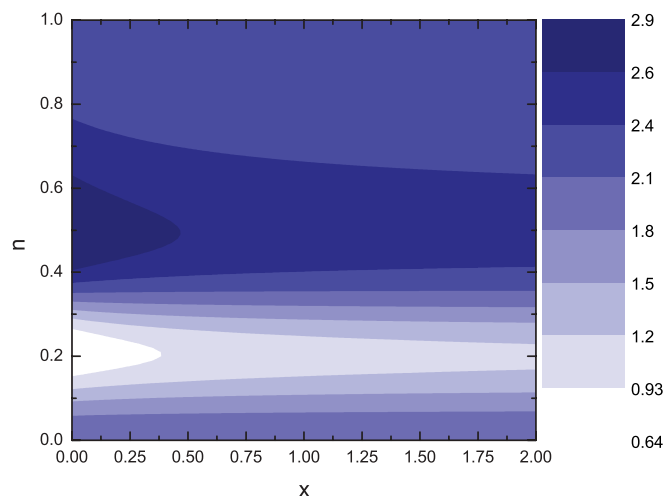where δz is $\delta\epsilon$ or δx.

FIG. 4. (Color online) Contour plot of $h_x(n,x)$ as a function of the magnetic field, represented by x, and the channel factor n. The color code is explained in the strip on the right-hand panel.

It is convenient to write the charge current covariance as a deformed Lorentzian. For parametric variations of z, we set $\mathrm{cov}[J_i^{(0)}(\epsilon,x), J_i^{(0)}(\epsilon,x')] = \alpha_z(n,x)/[1+(\delta x)^2]^{h_z(n,x)}$, where $\alpha_z(n,x)$ is a crossover function and $h_z(n,x)$ characterizes the Lorentzian shape deformation of the charge current correlation as a function of δx. In terms of the factor h_z, the average density of maxima reads

$$\langle\rho_z^{(\alpha)}\rangle = \frac{1}{2\pi}\sqrt{6[h_z(n,x)+1]}, \quad (23)$$

where z can be either ϵ or x.

Using Eqs. (20) and (23), we obtain an exact analytical expression for $h_x(n,x)$. Its explicit form is not presented here, since it is rather lengthy. Figure 4 illustrates its general features. For the unitary symmetry limit, it is well established[32,33] that the electronic conductance correlation function shows a square Lorentzian behavior. Accordingly, we find $h_{\mathrm{sqL}} \equiv \lim_{x\to\infty} h_x(n,x) = \lim_{x\to 0} h_x(n,x) = 2$ for the pure circular unitary and symplectic ensembles, respectively. The symplectic-unitary crossover shows a much richer behavior. Figure 4 exhibits a remarkable crossover between sub-Lorentzian, for which $h_x < 1$, with a minimum value of $h_x \approx 0.64$, and super-Lorentzian, for which $h_x > 1$ with a maximum value of $h_x \approx 2.92$.

Parametric variations of ϵ were first studied in nuclear scattering at low energies and known as Ericson fluctuations.[34] As is well known, their characteristic correlation function versus energy has a Lorentzian shape. In the presence of a perpendicular magnetic field and the channel factor, we obtained a unitary-symplectic crossover of Lorentzian-type shapes, generalizing the correlation functions of Ericson fluctuations. For parametric variations of ϵ, we set $\mathrm{cov}[J_i^{(0)}(\epsilon,x), J_i^{(0)}(\epsilon',x)] = \alpha_\epsilon(n,x)/[1+(\delta\epsilon)^2]^{h_\epsilon(n,x)}$, where $\alpha_\epsilon(n,x)$ is a crossover parameter and $h_\epsilon(n,x)$ characterizes the deformation of the Lorentzian shape. As in the previous case, we also obtain a lengthy analytical expression for $h_\epsilon(n,x)$. Its main features are displayed in Fig. 5. As expected, $h_{\mathrm{L}} \equiv \lim_{x\to\infty} h_\epsilon(n,x) = \lim_{x\to 0} h_\epsilon(n,x) = 1$, for pure circular unitary and symplectic ensembles, respectively. Figure 5 exhibits another remarkable
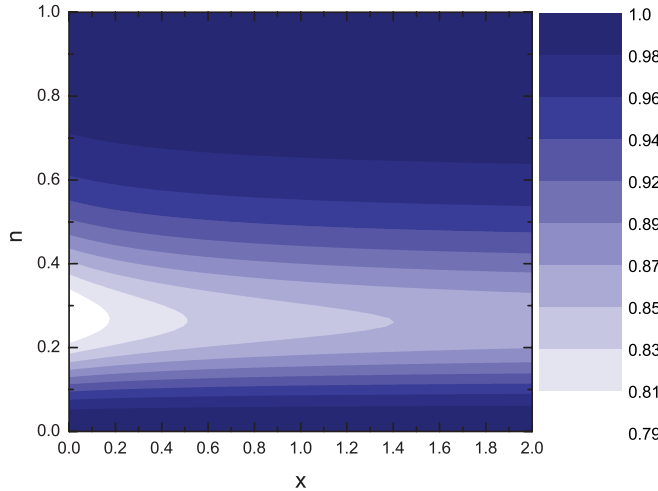
FIG. 5. (Color online) Contour plot of $h_\epsilon(n,x)$ as a function of the magnetic field, represented by x, and the channel factor n. The color code is explained in the strip on the right-hand panel.

crossover from a sub-Lorentzian, for which $h_\epsilon < 1$, to a Lorentzian behavior.

According to Eq. (23), the density of maxima corresponding to pure ensembles, namely, $x = 0$ or $x \gg 1$, is $\langle \rho_x^{(\alpha)} \rangle = \sqrt{6(h_{sqL} + 1)} \approx 0.68$ and $\langle \rho_\epsilon^{(\alpha)} \rangle = \sqrt{6(h_L + 1)} \approx 0.55$,[31,35] for both spin and charge currents. We emphasize that for the case of the spin correlation function, Eq. (19), $h_\epsilon = h_L = 1$ and $h_x = h_{sqL} = 2$ *even* in the crossover regime (any value of n and x).

Let us now focus on the longitudinal (charge) correlation function, Eq. (20). For a given value of the channel asymmetry factor, $\langle \rho_x^{(0)}(n,x) \rangle$ has a unique global maximum, $\langle \rho_x^{(0)}(n,x_{\max}) \rangle$, and minimum, $\langle \rho_x^{(0)}(n,x_{\min}) \rangle$ The difference, $\Delta\langle \rho_x(n) \rangle \equiv \langle \rho_x^{(0)}(n,x_{\max}) \rangle - \langle \rho_x^{(0)}(n,x_{\min}) \rangle$, increases with n until it saturates at $n \approx 3$. In the absence of spin leads, we find the difference $\Delta\langle \rho_x(0) \rangle \approx 0.27$. In the presence of spin leads,

we get $\Delta\langle \rho_x(0.5) \rangle \approx 0.19$, $\Delta\langle \rho_x(1) \rangle \approx 0.17$, $\Delta\langle \rho_x(2) \rangle \approx 0.15$, and $\Delta\langle \rho_x(5) \rangle \approx 0.14$. Thus, in measurements made with a perpendicular magnetic field, for symmetric channels ($n = 1$), the spin terminals lead to a reduction in the signal of about 37%, which becomes even larger with increasing n. Interestingly, the maximum and minimum of $\langle \rho_x \rangle$ correspond to magnetic field strengths $x_{\min} \approx 0.20$ and $x_{\max} \approx 0.47$, for $n \in [0,5]$, a rather narrow range of values which is accessible experimentally.

In contrast to $\langle \rho_x(n) \rangle$, the energy variation generates a density of conductance peaks containing a single global minimum, $\langle \rho_\epsilon(n,x_{\min}) \rangle$, and no global maximum. This minimum is located in a very narrow range of values of $x_{\min} \approx 0.26$ as a function of n. The minimum value of the density at these points is of the order of $\langle \rho_\epsilon \rangle \approx 0.52$.

V. SUMMARY AND CONCLUSION

In this paper, we have investigated the spin Hall conductance fluctuations in a chaotic open quantum dot with spin-orbit interaction. Both the electronic and the spin Hall conductance fluctuations are universal functions, with autocorrelation functions that depend on the magnitude of the external magnetic field B and the channel asymmetry factor n. A clear intermediate case of symplectic-unitary transitional behavior is found and can be tested experimentally. In particular, the spin current can be measured by using the charge current density of maxima. The results of this paper extend the understanding of mesoscopic fluctuations to spin and charge currents in the symplectic-unitary crossover, characteristic of quantum dots subjected to an external magnetic field.

[1]Y. K. Kato, R. C. Myers, A. C. Gossard, and D. D. Awschalom, Science **306**, 1910 (2004).

[2]S. O. Valenzuela and M. Tinkham, Nature (London) **442**, 176 (2006).

[3]T. Kimura, Y. Otani, T. Sato, S. Takahashi, and S. Maekawa, Phys. Rev. Lett. **98**, 156601 (2007).

[4]D. D. Awschalom and M. E. Flatté, Nat. Phys. **3**, 153 (2007).

[5]T. Jungwirth, J. Wunderlich, and K. Olejník, Nat. Mater. **11**, 382 (2012).

[6]J. E. Hirsch, Phys. Rev. Lett. **83**, 1834 (1999).

[7]J. Sinova, D. Culcer, Q. Niu, N. A. Sinitsyn, T. Jungwirth, and A. H. MacDonald, Phys. Rev. Lett. **92**, 126603 (2004).

[8]I. Zutić, J. Fabian, and S. Das Sarma, Rev. Mod. Phys. **76**, 323 (2004).

[9]J. Fabian, A. Matos-Abiaguea, C. Ertler, P. Stano, and I. Zutić, Acta Phys. Slovaca **57**, 565 (2007).

[10]J. G. G. S. Ramos, A. L. R. Barbosa, D. Bazeia, and M. S. Hussein, Phys. Rev. B **85**, 115123 (2012).

[11]W. Ren, Z. Qiao, J. Wang, Q. Sun, and H. Guo, Phys. Rev. Lett. **97**, 066603 (2006).

[12]J. H. Bardarson, I. Adagideli, and Ph. Jacquod, Phys. Rev. Lett. **98**, 196601 (2007).

[13]Y. V. Nazarov, New J. Phys. **9**, 352 (2007).

[14]J. J. Krich and B. I. Halperin, Phys. Rev. B **78**, 035338 (2008).

[15]P. W. Brouwer, J. N. H. J. Cremers, and B. I. Halperin, Phys. Rev. B **65**, 081302(R) (2002).

[16]J.-H. Cremers, P. W. Brouwer, and V. I. Falko, Phys. Rev. B **68**, 125329 (2003).

[17]I. Adagideli, J. H. Bardarson, and P. Jacquod, J. Phys.: Condens. Matter **21**, 155503 (2009).

[18]P. Jacquod, R. S. Whitney, J. Meair, and M. Büttiker, Phys. Rev. B **86**, 155118 (2012).

[19]M. Büttiker, Phys. Rev. Lett. **57**, 1761 (1986).

[20]C. W. J. Beenakker, Rev. Mod. Phys. **69**, 731 (1997).

[21]Y. Alhassid, Rev. Mod. Phys. **72**, 895 (2000).

[22]P. W. Brouwer and C. W. J. Beenakker, J. Math. Phys. **37**, 4904 (1996).

[23]M. L. Mehta, *Random Matrices* (Academic, New York, 1991).

[24]Z. Pluhař, H. A. Weidenmüller, J. A. Zuk, C. H. Lewenkopf, and F. J. Wegner, Ann. Phys. (NY) **243**, 1 (1995).

[25]J. G. G. S. Ramos, A. L. R. Barbosa, and A. M. S. Macêdo, Phys. Rev. B **84**, 035453 (2011).

[26]For a review, see *Mesoscopic Phenomena in Solids*, edited by B. L. Altshuler, P. A. Lee, and R. A. Webb (North-Holland, Amsterdam, 1991).

[27]C. Mahaux and H. A. Weidenmüller, *Shell Model Approach to Nuclear Reactions* (North-Holland, Amsterdam, 1969).

[28]C. H. Lewenkopf and H. A. Weidenmüller, Ann. Phys. (NY) **212**, 53 (1991).

[29]J. J. M. Verbaarschot, H. A. Weidenmüller, and M. R. Zirnbauer, Phys. Rep. **129**, 367 (1985).

[30]A. L. R. Barbosa, J. G. G. S. Ramos, and D. Bazeia, Phys. Rev. B **84**, 115312 (2011).

[31]J. G. G. S. Ramos, D. Bazeia, M. S. Hussein, and C. H. Lewenkopf, Phys. Rev. Lett. **107**, 176807 (2011).

[32]K. B. Efetov, Phys. Rev. Lett. **74**, 2299 (1995).

[33]R. O. Vallejos and C. H. Lewenkopf, J. Phys. A **34**, 2713 (2001); E. R. P. Alves and C. H. Lewenkopf, Phys. Rev. Lett. **88**, 256805 (2002).

[34]T. Ericson, Ann. Phys. (NY) **23**, 390 (1963).

[35]D. M. Brink and R. O. Stephen, Phys. Lett. **5**, 77 (1963).